Finite Energy One-Half Monopole Solutions of the SU(2) Yang-Mills-Higgs Theory

Rosy Teh[1], Ban-Loong Ng and Khai-Ming Wong

School of Physics
Universiti Sains Malaysia

5 July 2012
36th International Conference on High Energy Physics
Melbourne Convention and Exhibition Centre, Melbourne, Australia
July 4 - 11, 2012

[1]speaker, email:rosyteh@usm.my

Outline

Abstract

- We present finite energy SU(2) Yang-Mills-Higgs particles of one-half topological charge.
- The 't Hooft Abelian magnetic fields of these solutions at spatial infinity correspond to the magnetic field of a positive one-half magnetic monopole located at $r = 0$ and a semi-infinite Dirac string singularity located on one half of the z-axis which carries a magnetic flux of $\frac{2\pi}{g}$ going into the center of the sphere at infinity. Hence the net magnetic charge is zero.
- The non-Abelian solutions possess gauge potentials that are singular at only one point at large distances, elsewhere they are regular.

The SU(2) YMH Theory

- The SU(2) YMH Lagrangian is given by

$$\mathcal{L} = -\frac{1}{4}F^a_{\mu\nu}F^{a\mu\nu} - \frac{1}{2}D^\mu\Phi^a D_\mu\Phi^a - \frac{1}{4}\lambda(\Phi^a\Phi^a - \frac{\mu^2}{\lambda})^2. \qquad (1)$$

  Here μ is the Higgs field mass, λ is the strength of the Higgs potential. The vacuum expectation value of the Higgs field is $\xi = \mu/\sqrt{\lambda}$.

- The covariant derivative of the Higgs field and the gauge field strength tensor are given respectively by

$$\begin{aligned} D_\mu\Phi^a &= \partial_\mu\Phi^a + g\epsilon^{abc}A^b_\mu\Phi^c, \\ F^a_{\mu\nu} &= \partial_\mu A^a_\nu - \partial_\nu A^a_\mu + g\epsilon^{abc}A^b_\mu A^c_\nu, \end{aligned} \qquad (2)$$

  where g is the gauge field coupling constant. The metric used is $g_{\mu\nu} = (-+++)$. The SU(2) internal group indices $a, b, c = 1, 2, 3$ and the space-time indices are $\mu, \nu, \alpha = 0, 1, 2,$ and 3 in Minkowski space.

The SU(2) YMH Theory (cont.)

- The equations of motion that follow from the Lagrangian (1) are

$$\begin{aligned} D^\mu F^a_{\mu\nu} &= \partial^\mu F^a_{\mu\nu} + g\epsilon^{abc} A^{b\mu} F^c_{\mu\nu} = g\epsilon^{abc}\Phi^b D_\nu \Phi^c, \\ D^\mu D_\mu \Phi^a &= \lambda\Phi^a(\Phi^b\Phi^b - \xi^2), \end{aligned} \tag{3}$$

  and the Bogomol'nyi equation holds in the limit of vanishing μ and λ,

$$B^a_i \pm D_i\Phi^a = 0. \tag{4}$$

- The electromagnetic field tensor proposed by 't Hooft [1] is

$$\begin{aligned} F_{\mu\nu} &= \hat{\Phi}^a F^a_{\mu\nu} - \frac{1}{g}\epsilon^{abc}\hat{\Phi}^a D_\mu \hat{\Phi}^b D_\nu \hat{\Phi}^c, \\ &= \partial_\mu A_\nu - \partial_\nu A_\mu - \frac{1}{g}\epsilon^{abc}\hat{\Phi}^a \partial_\mu \hat{\Phi}^b \partial_\nu \hat{\Phi}^c, \end{aligned} \tag{5}$$

  where $A_\mu = \hat{\Phi}^a A^a_\mu$, the Higgs unit vector, $\hat{\Phi}^a = \Phi^a/|\Phi|$, and the Higgs field magnitude $|\Phi| = \sqrt{\Phi^a\Phi^a}$.

The SU(2) YMH Theory (cont.)

- Eq. (5) can be decompose into the gauge part and the Higgs part respectively,

$$G_{\mu\nu} = \partial_\mu A_\nu - \partial_\nu A_\mu, \quad H_{\mu\nu} = -\frac{1}{g}\epsilon^{abc}\hat{\Phi}^a \partial_\mu \hat{\Phi}^b \partial_\nu \hat{\Phi}^c. \tag{6}$$

- Hence the decomposed magnetic field is

$$B_i = -\frac{1}{2}\epsilon_{ijk} F_{jk} = B_i^G + B_i^H. \tag{7}$$

The net magnetic charge of the system is

$$M = \frac{1}{4\pi}\int \partial^i B_i \; d^3x = \frac{1}{4\pi}\oint d^2\sigma_i \; B_i. \tag{8}$$

The SU(2) YMH Theory (cont.)

- The topological magnetic current [12]

$$k_\mu = \frac{1}{8\pi}\,\epsilon_{\mu\nu\rho\sigma}\;\epsilon_{abc}\;\partial^\nu\hat{\Phi}^a\;\partial^\rho\hat{\Phi}^b\;\partial^\sigma\hat{\Phi}^c, \tag{9}$$

is also the topological current density of the system. Hence the corresponding conserved topological magnetic charge is

$$\begin{aligned} M_H &= \frac{1}{g}\int d^3x\; k_0 = \frac{1}{8\pi g}\int \epsilon_{ijk}\epsilon^{abc}\partial_i\left(\hat{\Phi}^a\partial_j\hat{\Phi}^b\partial_k\hat{\Phi}^c\right)d^3x \\ &= \frac{1}{8\pi}\oint d^2\sigma_i\left(\frac{1}{g}\epsilon_{ijk}\epsilon^{abc}\hat{\Phi}^a\partial_j\hat{\Phi}^b\partial_k\hat{\Phi}^c\right) \\ &= \frac{1}{4\pi}\oint d^2\sigma_i\; B_i^H. \end{aligned} \tag{10}$$

The magnetic charge M_H is the total magnetic charge of the system if and only if the gauge field is non singular [13]. If the gauge field is singular and carries Dirac string monopoles M_G, then the total magnetic charge is $M = M_G + M_H$.

The SU(2) YMH Theory (cont.)

- In the electrically neutral BPS limit when the Higgs potential vanishes, the energy is a minimum, [14]

$$\begin{aligned} E_{min} &= \mp \int \partial_i (B_i^a \Phi^a)\, d^3x + \int \frac{1}{2}(B_i^a \pm D_i \Phi^a)^2\, d^3x \\ &= \mp \int \partial_i (B_i^a \Phi^a)\, d^3x = \frac{4\pi\xi}{g} M_H. \end{aligned} \tag{11}$$

  Hence the dimensionless minimum total energy is M_H.

- For non-BPS solution, its energy must be greater than that of Eq. (11). The dimensionless value is given by

$$E = \frac{g}{8\pi\xi} \int \{B_i^a B_i^a + D_i \Phi^a D_i \Phi^a + \frac{\lambda}{2}(\Phi^a \Phi^a - \xi^2)^2\}\, d^3x \geq M_H. \tag{12}$$

The SU(2) YMH Theory (cont.)

- The magnetic ansatz is [8]

$$\begin{aligned} gA_i^a &= -\frac{\hat{n}_\phi^a}{r}\left\{\psi_1(r,\theta)\hat{\theta}_i - R_1(r,\theta)\hat{r}_i\right\} + \frac{1}{r\sin\theta}\left\{P_1(r,\theta)\hat{n}_\theta^a - P_2(r,\theta)\hat{n}_r^a\right\}\hat{\phi}_i, \\ gA_0^a &= 0, \quad g\Phi^a = \Phi_1(r,\theta)\ \hat{n}_r^a + \Phi_2(r,\theta)\hat{n}_\theta^a, \end{aligned} \tag{13}$$

where $P_1(r,\theta) = \sin\theta\ \psi_2(r,\theta)$ and $P_2(r,\theta) = \sin\theta\ R_2(r,\theta)$. The spatial and isospin unit vectors are respectively,

$$\begin{aligned} \hat{r}_i &= \sin\theta\ \cos\phi\ \delta_{i1} + \sin\theta\ \sin\phi\ \delta_{i2} + \cos\theta\ \delta_{i3}, \\ \hat{\theta}_i &= \cos\theta\ \cos\phi\ \delta_{i1} + \cos\theta\ \sin\phi\ \delta_{i2} - \sin\theta\ \delta_{i3}, \\ \hat{\phi}_i &= -\sin\phi\ \delta_{i1} + \cos\phi\ \delta_{i2}, \end{aligned} \tag{14}$$

$$\begin{aligned} \hat{n}_r^a &= \sin\theta\ \cos n\phi\ \delta_1^a + \sin\theta\ \sin n\phi\ \delta_2^a + \cos\theta\ \delta_3^a, \\ \hat{n}_\theta^a &= \cos\theta\ \cos n\phi\ \delta_1^a + \cos\theta\ \sin n\phi\ \delta_2^a - \sin\theta\ \delta_3^a, \\ \hat{n}_\phi^a &= -\sin n\phi\ \delta_1^a + \cos n\phi\ \delta_2^a; \quad \text{where} \quad n = 1. \end{aligned} \tag{15}$$

The SU(2) YMH Theory (cont.)

- The magnetic ansatz (13) is form invariant under the gauge transformation

$$\omega = \exp\left(\frac{i}{2}\sigma^a \hat{n}^a_\phi f(r,\theta)\right), \quad \sigma^a = \text{ Pauli matrices} \tag{16}$$

and the transformed gauge potential and Higgs field take the form,

$$\begin{aligned}
gA'^a_i &= -\frac{1}{r}\{\psi_1 - \partial_\theta f\}\hat{n}^a_\phi \hat{\theta}_i + \frac{1}{r}\{R_1 + r\partial_r f\}\hat{n}^a_\phi \hat{r}_i \\
&+ \frac{1}{r\sin\theta}\{P_1\cos f + P_2 \sin f + n[\sin\theta - \sin(f+\theta)]\}\,\hat{n}^a_\theta \hat{\phi}_i \\
&- \frac{1}{r\sin\theta}\{P_2\cos f - P_1 \sin f + n[\cos\theta - \cos(f+\theta)]\}\,\hat{n}^a_r \hat{\phi}_i, \\
gA'^a_0 &= 0, \\
g\Phi'^a &= (\Phi_1\cos f + \Phi_2 \sin f)\ \hat{n}^a_r + (\Phi_2\cos f - \Phi_1 \sin f)\hat{n}^a_\theta.
\end{aligned} \tag{17}$$

The SU(2) YMH Theory (cont.)

- The general Higgs fields in the spherical and the rectangular coordinate systems are respectively

$$\begin{aligned} g\Phi^a &= \Phi_1(x)\ \hat{n}_r^a + \Phi_2(x)\hat{n}_\theta^a + \Phi_3(x)\hat{n}_\phi^a \\ &= \tilde{\Phi}_1(x)\ \delta^{a1} + \tilde{\Phi}_2(x)\ \delta^{a2} + \tilde{\Phi}_3(x)\ \delta^{a3}, \qquad (18) \\ \tilde{\Phi}_1 &= \sin\theta\cos n\phi\ \Phi_1 + \cos\theta\cos n\phi\ \Phi_2 - \sin n\phi\ \Phi_3 = |\Phi|\sin\alpha\cos\beta \\ \tilde{\Phi}_2 &= \sin\theta\sin n\phi\ \Phi_1 + \cos\theta\sin n\phi\ \Phi_2 + \cos n\phi\ \Phi_3 = |\Phi|\sin\alpha\sin\beta \\ \tilde{\Phi}_3 &= \cos\theta\ \Phi_1 - \sin\theta\ \Phi_2 = |\Phi|\cos\alpha. \qquad (19) \end{aligned}$$

The axially symmetric Higgs unit vector in rectangular coordinate system is

$$\begin{aligned} \hat{\Phi}^a &= \sin\alpha\cos\beta\ \delta^{a1} + \sin\alpha\sin\beta\ \delta^{a2} + \cos\alpha\ \delta^{a3},\ \beta = n\phi, \qquad (20) \\ \cos\alpha &= g\cos\theta - h\sin\theta,\ g = \frac{\Phi_1}{|\Phi|},\ h = \frac{\Phi_2}{|\Phi|}. \qquad (21) \end{aligned}$$

The SU(2) YMH Theory (cont.)

- Hence the Higgs part and the gauge part of the 't Hooft magnetic field (7) become

$$gB_i^H = -n\epsilon_{ijk}\partial^j \cos\alpha \partial^k \phi \tag{22}$$

$$gB_i^G = -n\epsilon_{ijk}\partial_j \cos\kappa\ \partial_k\phi,\ \ \cos\kappa = \frac{1}{n}\left(hP_1 - gP_2\right), \tag{23}$$

and the 't Hooft's magnetic field is

$$gB_i = -n\epsilon_{ijk}\partial_j(\cos\alpha + \cos\kappa)\ \partial_k\phi = -\epsilon_{ijk}\partial_j\mathcal{A}_k, \tag{24}$$

where $\mathcal{A}_i$ is the 't Hooft's gauge potential.

- The orientation of the magnetic field can be plotted by using the vector plot of the magnetic field unit vector,

$$\hat{B}_i = \frac{-\partial_\theta(\cos\alpha + \cos\kappa)\hat{r}_i + r\partial_r(\cos\alpha + \cos\kappa)\hat{\theta}_i}{\sqrt{[r\partial_r(\cos\alpha + \cos\kappa)]^2 + [\partial_\theta(\cos\alpha + \cos\kappa)]^2}}. \tag{25}$$

The SU(2) YMH Theory (cont.)

- We also note that the Higgs field (13) and the gauge transformed Higgs field (17) can be simplified to

$$\begin{aligned} \Phi^a &= |\Phi|(\cos(\alpha-\theta)\ \hat{n}_r^a + \sin(\alpha-\theta)\hat{n}_\theta^a), \\ \Phi'^a &= |\Phi|(\cos(\alpha'-\theta)\ \hat{n}_r^a + \sin(\alpha'-\theta)\hat{n}_\theta^a),\ \alpha' = \alpha - f. \end{aligned} \tag{26}$$

- At spatial infinity, all non-Abelian components of the gauge potential vanish and the electromagnetic field tends to

$$F_{\mu\nu}^a\big|_{r\to\infty} = \{\partial_\mu A_\nu - \partial_\nu A_\mu - \frac{1}{g}\epsilon^{cde}\hat{\Phi}^c\partial_\mu\hat{\Phi}^d\partial_\nu\hat{\Phi}^e\}\hat{\Phi}^a = F_{\mu\nu}\hat{\Phi}^a, \tag{27}$$

  where $F_{\mu\nu}$ is the 't Hooft electromagnetic field.
- However there is no unique way of representing the Abelian electromagnetic field in the region at finite values of r [15]. One proposal was given by 't Hooft as in Eq. (5).
- Another proposal which is less singular was given by Bogomol'nyi [3] and Faddeev [16],

$$\mathcal{B}_i = B_i^a\left(\frac{\Phi^a}{\xi}\right), \quad \mathcal{E}_i = E_i^a\left(\frac{\Phi^a}{\xi}\right). \tag{28}$$

The Exact Asymptotic One-Half Monopole Solutions

- We start by analysing four seemingly different types of one-half monopole charge solutions that we label as Type $A1$, $A2$, $B1$, and $B2$.
- The profile functions of the non-Abelian gauge potentials (13) of the four types of one-half monopole solution at r infinity are given respectively by,

$$\begin{aligned}
\text{(Type } A1) \quad \psi_1 &= \frac{1}{2}, \quad P_1 = \sin\theta - \frac{1}{2}\sin\frac{1}{2}\theta(1+\cos\theta), \\
R_1 &= 0, \quad P_2 = \cos\theta - \frac{1}{2}\cos\frac{1}{2}\theta(1+\cos\theta), \\
\Phi_1 &= \xi\cos\frac{1}{2}\theta, \quad \Phi_2 = -\xi\sin\frac{1}{2}\theta. \qquad (29) \\
\text{(Type } A2) \quad \psi_1 &= -\frac{1}{2}, \quad P_1 = \sin\theta - \frac{1}{2}\sin\frac{3}{2}\theta(1+\cos\theta), \\
R_1 &= 0, \quad P_2 = \cos\theta - \frac{1}{2}\cos\frac{3}{2}\theta(1+\cos\theta), \\
\Phi_1 &= \xi\cos\frac{3}{2}\theta, \quad \Phi_2 = -\xi\sin\frac{3}{2}\theta. \qquad (30) \\
\text{(Type } B1) \quad \psi_1 &= \frac{1}{2}, \quad P_1 = \sin\theta - \frac{1}{2}\cos\frac{1}{2}\theta(1-\cos\theta),
\end{aligned}$$

The Exact Asymptotic One-Half Monopole Solutions (cont.)

$$\begin{aligned} & R_1 = 0, \quad P_2 = \cos\theta + \frac{1}{2}\sin\frac{1}{2}\theta(1-\cos\theta), \\ & \Phi_1 = \xi\sin\frac{1}{2}\theta, \quad \Phi_2 = \xi\cos\frac{1}{2}\theta. \end{aligned} \tag{31}$$

$$\begin{aligned} \text{(Type } B2) \quad & \psi_1 = -\frac{1}{2}, \quad P_1 = \sin\theta + \frac{1}{2}\cos\frac{3}{2}\theta(1-\cos\theta), \\ & R_1 = 0, \quad P_2 = \cos\theta - \frac{1}{2}\sin\frac{3}{2}\theta(1-\cos\theta), \\ & \Phi_1 = -\xi\sin\frac{3}{2}\theta, \quad \Phi_2 = -\xi\cos\frac{3}{2}\theta. \end{aligned} \tag{32}$$

- The Type A (Type B) solutions possess 't Hooft's gauge potential, which is singular along the positive (negative) z-axis,

$$\mathcal{A}_i = \left\{ \frac{\cos\theta \pm 1}{2r\sin\theta} \right\} \hat{\phi}_i. \tag{33}$$

The Exact Asymptotic One-Half Monopole Solutions (cont.)

- The Higgs magnetic fields are given by

$$gB_i^H = \frac{\frac{1}{2}\sin(\frac{1}{2}\theta)}{\sin\theta}\frac{\hat{r}_i}{r^2}, \qquad \text{Type } A \text{ solutions}, \tag{34}$$

$$gB_i^H = \frac{\frac{1}{2}\cos(\frac{1}{2}\theta)}{\sin\theta}\frac{\hat{r}_i}{r^2}, \qquad \text{Type } B \text{ solutions}, \tag{35}$$

  and the net 't Hooft's magnetic fields are given by

$$gB_i = \frac{\hat{r}_i}{2r^2} - 2\pi\delta(x_1)\delta(x_2)\theta(x_3)\delta_i^3, \qquad \text{Type } A \text{ solutions}, \tag{36}$$

$$gB_i = \frac{\hat{r}_i}{2r^2} + 2\pi\delta(x_1)\delta(x_2)\theta(-x_3)\delta_i^3, \qquad \text{Type } B \text{ solutions}. \tag{37}$$

- The solutions therefore carry a positive one-half monopole at the origin and the semi-infinite Dirac string singularity carries the other opposite half of the magnetic monopole charge. Hence the net magnetic charge of the configuration is zero.

The Numerical Calculations

- The numerical one-half monopole solutions are constructed by using the exact asymptotic solutions at large distances (29) - (32) for the Type $A1$, $A2$, $B1$, and $B2$ solutions respectively and by fixing the boundary conditions for all the profile functions (13) along the z-axis and near $r = 0$.
- In order to avoid the singularity of $R_2(r, \theta)$, we choose to perform our numerical analysis with the functions,

$$P_1(r, \theta) = \psi_2(r, \theta) \sin\theta, \quad P_2(r, \theta) = R_2(r, \theta) \sin\theta. \tag{38}$$

- Near $r = 0$, we have the common trivial vacuum solution for all the four solutions. The asymptotic solutions and boundary conditions at small distances that will give rise to finite energy solutions are

$$\psi_1 = P_1 = R_1 = P_2 = 0, \quad \Phi_1 = \xi_0 \cos\theta, \quad \Phi_2 = -\xi_0 \sin\theta, \tag{39}$$

$$\sin\theta\Phi_1(0, \theta) + \cos\theta\Phi_2(0, \theta) = 0,$$

$$\partial_r(\cos\theta\Phi_1(r, \theta) - \sin\theta\Phi_2(r, \theta))|_{r=0} = 0. \tag{40}$$

The Numerical Calculations (cont.)

- The boundary conditions imposed along the positive z-axis for the profile functions (13) of the Type A solutions are

$$\partial_\theta \Phi_1(r,\theta)|_{\theta=0} = 0, \quad \Phi_2(r,0) = 0, \quad \partial_\theta \psi_1(r,\theta)|_{\theta=0} = 0,$$
$$R_1(r,0) = 0, \quad P_1(r,0) = 0, \quad P_2(r,0) = 0. \tag{41}$$

Along the negative z-axis, the boundary conditions imposed are

$$\Phi_1(r,\pi) = 0, \quad \partial_\theta \Phi_2(r,\theta)|_{\theta=\pi} = 0, \quad \partial_\theta \psi_1(r,\theta)|_{\theta=\pi} = 0,$$
$$R_1(r,\pi) = 0, \quad P_1(r,\pi) = 0, \quad \partial_\theta P_2(r,\theta)|_{\theta=\pi} = 0. \tag{42}$$

- The boundary conditions imposed along the positive z-axis for the profile functions (13) of the Type B solutions are

$$\Phi_1(r,0) = 0, \quad \partial_\theta \Phi_2(r,\theta)|_{\theta=0} = 0, \quad \partial_\theta \psi_1(r,\theta)|_{\theta=0} = 0,$$
$$R_1(r,0) = 0, \quad P_1(r,0) = 0, \quad \partial_\theta P_2(r,\theta)|_{\theta=0} = 0, \tag{43}$$

and along the negative z-axis, the boundary conditions imposed are

$$\partial_\theta \Phi_1(r,\theta)|_{\theta=\pi} = 0, \quad \Phi_2(r,\pi) = 0, \quad \partial_\theta \psi_1(r,\theta)|_{\theta=\pi} = 0,$$
$$R_1(r,\pi) = 0, \quad P_1(r,\pi) = 0, \quad P_2(r,\pi) = 0. \tag{44}$$

The Numerical Calculations (cont.)

- We set $\xi = 1$, $g = 1$ and $0 \leq \lambda = \mu \leq 12$. The numerical solutions connecting the asymptotic solutions (29)-(32) at large r to the trivial vacuum solution (39) at small r and subjected to the boundary conditions (40)-(42) for the Type A solutions and the boundary conditions (40), (43)-(44) for the Type B solutions together with the gauge fixing condition [8]

$$r\partial_r R_1 - \partial_\theta \psi_1 = 0, \tag{45}$$

  are solved using the Maple 12 and MatLab R2009a softwares [19].
- The second order equations of motion (3) which are reduced to six partial differential equations with the ansatz (13) are then transformed into a system of nonlinear equations using the finite difference approximation.
- The system of nonlinear equations are discretized on a non-equidistant grid of size 90×80 covering the integration regions $0 \leq \bar{x} \leq 1$ and $0 \leq \theta \leq \pi$. Here $\bar{x} = \frac{r}{r+1}$ is the finite interval compactified coordinate. The partial derivative with respect to the radial coordinate is then replaced accordingly by $\partial_r \to (1-\bar{x})^2 \partial_{\bar{x}}$ and $\frac{\partial^2}{\partial r^2} \to (1-\bar{x})^4 \frac{\partial^2}{\partial \bar{x}^2} - 2(1-\bar{x})^3 \frac{\partial}{\partial \bar{x}}$. The numerical overall error estimate is 10^{-4}.

The Magnetic Dipole Moment and Magnetic Charge

- The profile functions, $\psi_1, P_1, R_1, P_2, \Phi_1$, and Φ_2 of the one-half monopole solutions are regular functions of r and θ. However the function $R_2 = \frac{P_2}{\sin\theta}$ possesses only one singular point at infinity (negative z-axis - Type A, positive z-axis - Type B).
- The 't Hooft's gauge potential at large r, tends to

$$\mathcal{A}_i = (\cos\alpha + \cos\kappa)\partial_i\phi|_{r\to\infty} = \frac{\hat{\phi}_i}{r\sin\theta}\left(\frac{1}{2}(\cos\theta \pm 1) + \frac{F_G(\theta)}{r}\right), \quad (46)$$

$$F_G(\theta) = r(h(P_1 - \sin\theta) - g(P_2 - \cos\theta) - \frac{1}{2}(\cos\theta \pm 1))|_{r\to\infty}, \quad (47)$$

  for the Type A and Type B solutions respectively.
- From the graphs of $F_G(\theta)$ versus angle θ, we find that $F_G(\theta) = \mu_m \sin^2\theta$, where μ_m is the dimensionless magnetic dipole moment of the one-half monopole and is non vanishing for all values of λ.
- In the limit when $\lambda = 0$, $\mu_m = \pm 1.32$ for the Type 1 solutions and $\mu_m = \pm 1.04$ for the Type 2 solutions. Figure 1 (a).

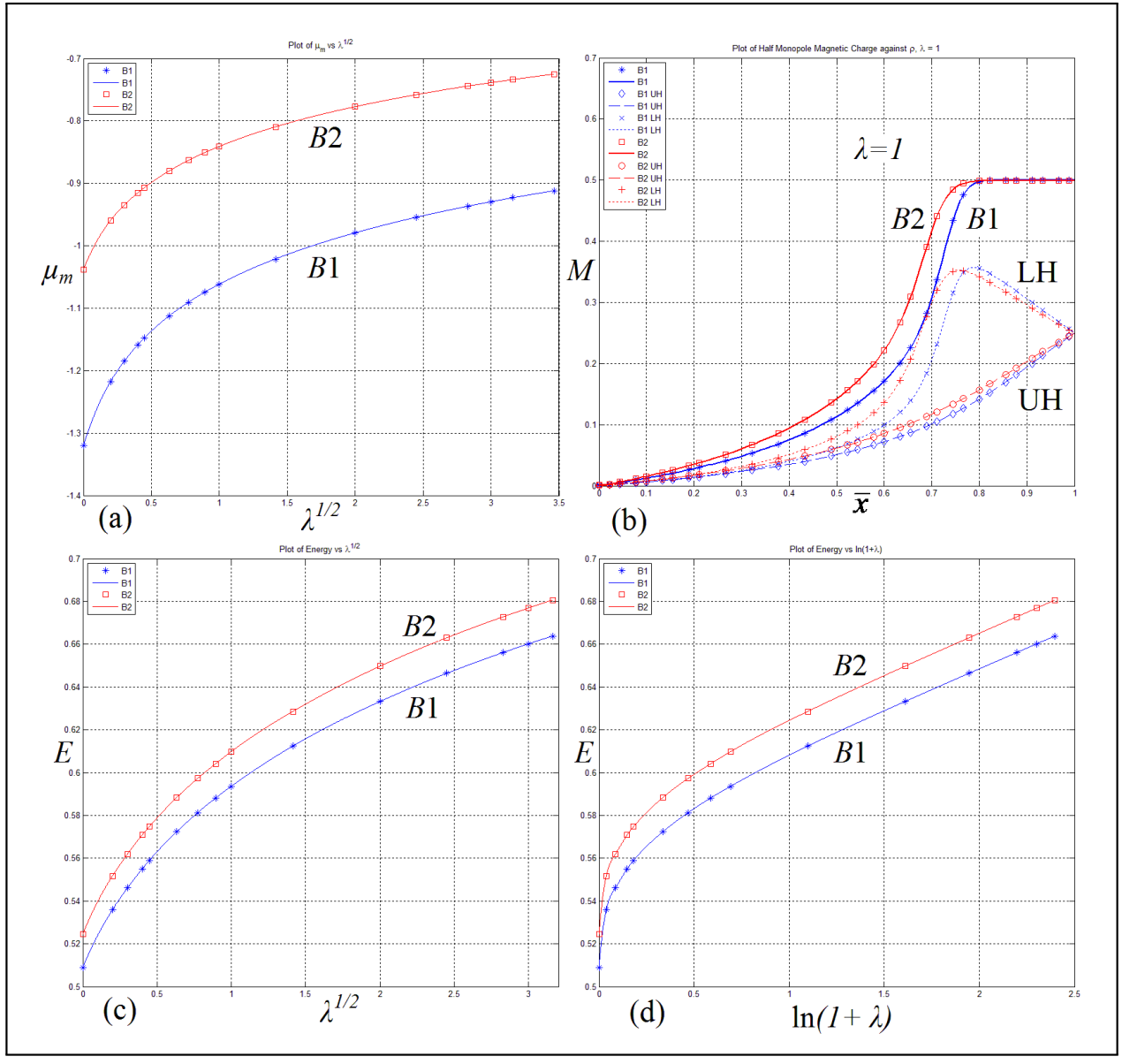

Figure 1: (a) Plot of μ_m versus $\lambda^{1/2}$. (b) Plot of M versus $\bar{x}$. (UH = upper hemisphere, LH = lower hemisphere). Plots of E versus (c) $\lambda^{1/2}$ and (d) $\ln(1+\lambda)$. Here $g = \xi = 1$.

The Magnetic Dipole Moment and Magnetic Charge

- The net magnetic charge M (8) of the one-half monopole configurations are plotted numerically versus the compactified axis, $\bar{x}$, when $\lambda = \xi = 1$. Figure 1 (b). We notice that $M = \frac{1}{2}$ when $r \geq 4$ and its value vanishes as r tends to zero.
- Also plotted in Figure 1 (b) are the magnetic charges covered by the upper hemisphere and lower hemisphere versus $\bar{x}$. The plots show that the magnetic charge at the origin is 'heavier' on the side of the z-axis away from the Dirac string.
- Using the definition (28) by Bogomol'nyi [3] and Faddeev [16], we can write

$$M = \frac{1}{4\pi} \int \partial^i \mathcal{B}_i \; d^3x = \int \mathcal{M} \; d\theta \; dr, \quad \mathcal{M} = \frac{1}{2} r^2 \sin\theta \{\partial^i \mathcal{B}_i\}, \tag{48}$$

where $\mathcal{M}$ is the magnetic charge density. Figure 2.

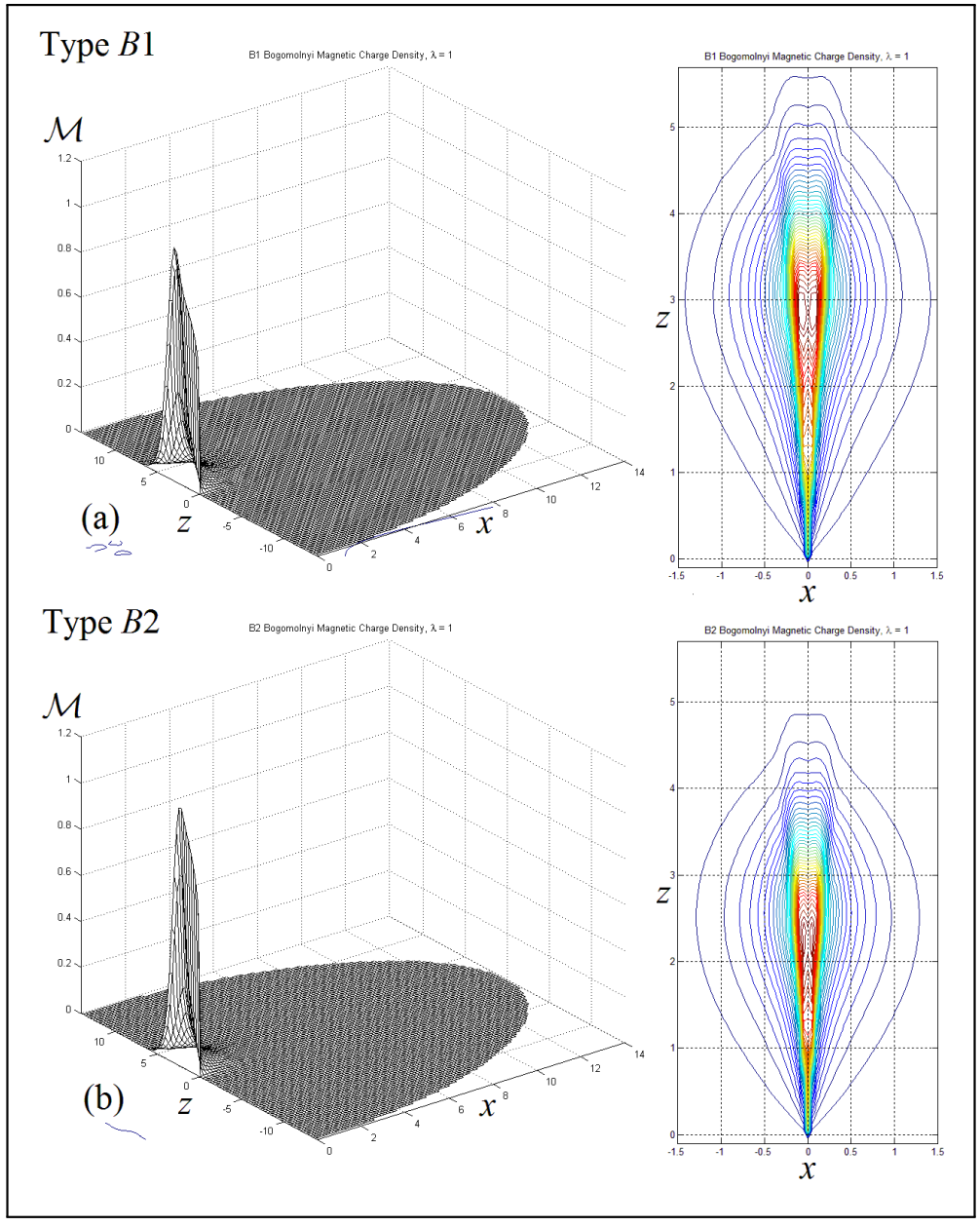

Figure 2: 3D surface and contour plots of the magnetic charge density $\mathcal{M}$ of the (a) Type $B1$ and (b) Type $B2$ one-half monopole solutions along the x-z plane at $y = 0$ when $\lambda = \xi = 1$.

The Magnetic Dipole Moment and Magnetic Charge

	Type 1	Type 2	Type 1	Type 2
λ	μ_m	μ_m	E	E
0	± 1.3203	± 1.0383	0.5090	0.5245
0.04	± 1.2173	± 0.9592	0.5360	0.5518
0.20	± 1.1480	± 0.9073	0.5589	0.5747
0.40	± 1.1124	± 0.8801	0.5723	0.5883
0.60	± 1.0904	± 0.8631	0.5813	0.5973
0.80	± 1.0743	± 0.8507	0.5881	0.6041
1.00	± 1.0616	± 0.8409	0.5936	0.6098
2.00	± 1.0211	± 0.8095	0.6124	0.6286
4.00	± 0.9793	± 0.7772	0.6332	0.6497
8.00	± 0.9367	± 0.7443	0.6561	0.6728
12.00	± 0.9242	± 0.7297	0.6702	0.6862

Table 1: Table of the dimensionless magnetic dipole moment μ_m and dimensionless total energy E of the Type 1 and Type 2 solutions for different values of λ. The magnetic dipole moment μ_m is positive for the Type A solutions and negative for the Type B solutions.

The Magnetic Field and Higgs Field

- From Eq. (24), the magnetic field lines contour plots of the one-half monopole solutions along the x-z plane at $y = 0$ when $\lambda = \xi = 1$ are shown in Figure 3.
- The direction of the magnetic field lines are shown in the vector field plot of the magnetic field unit vector $\hat{B}_i$ (25) of the one-half monopole solutions along the x-z plane at $y = 0$ when $\lambda = \xi = 1$. The * indicates the location of the one-half monopole. The presence of a one-half monopole sitting at $r = 0$ is once again indicated by the location of the Higgs field's node marked * on the Higgs field's vector plots along the x-z plane at $y = 0$. Figure 3.
- The 3D surface and contour plots of the modulus of the Higgs field $|\Phi|$ of the one-half monopole solutions along the x-z plane at $y = 0$ when $\lambda = \xi = 1$, show that there is a point zero of the Higgs field modulus at $r = 0$ where the one-half monopole is located. Figure 4.

The Magnetic Field and Higgs Field (cont.)

- The modulus of the Higgs field at large r tends to

$$g|\Phi(r,\theta)|_{r\to\infty} = (\xi - \frac{F_H(\theta)}{r}). \tag{49}$$

We find that $F_H(\theta)$ is a non vanishing constant c_1 only when $\lambda = 0$. $c_1 = -0.43$ (Type 1) and $c_1 = -0.63$ (Type 2). For non vanishing values of λ, $c_1 = 0$ for the one-half monopole solutions.

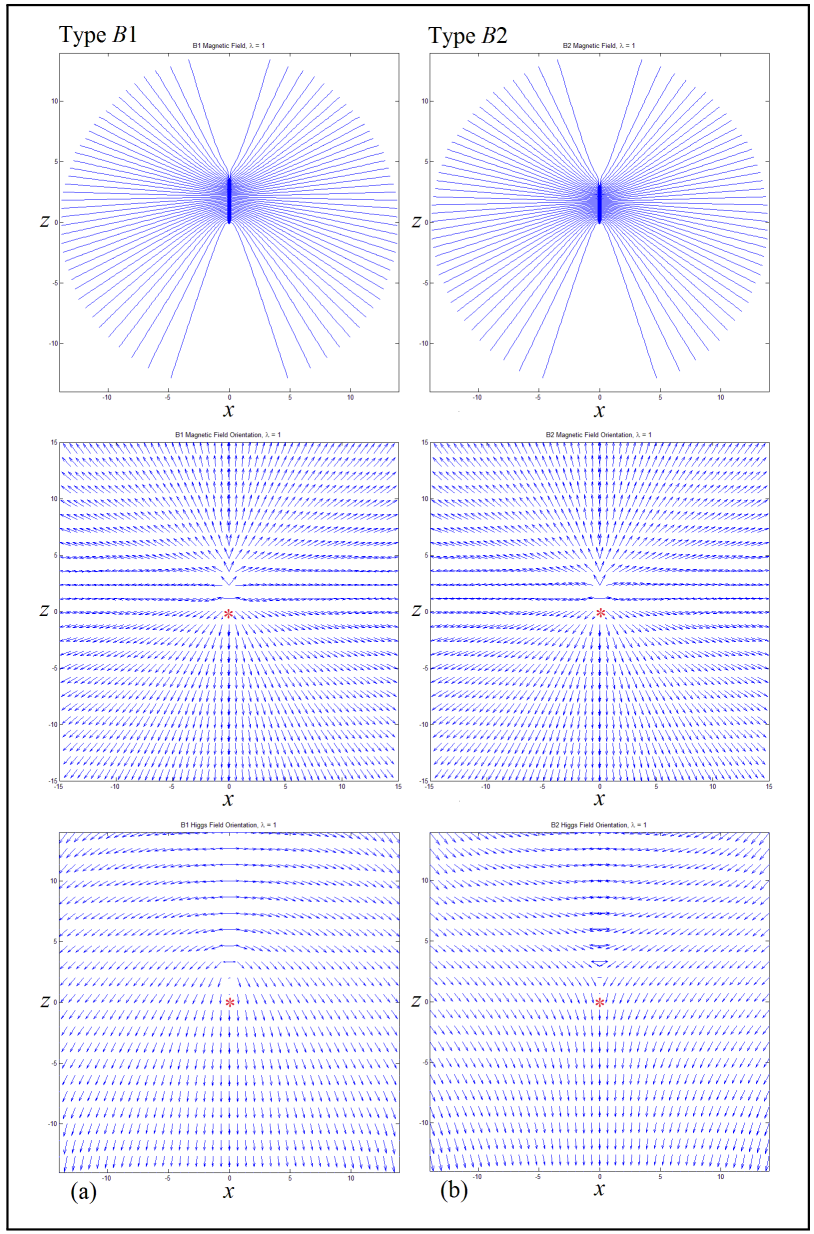

Figure 3: Contour plot of the 't Hooft magnetic field lines, unit vector field plot of the 't Hooft magnetic field and Higgs field vector plots of the (a) Type $B1$ and (b) Type $B2$ solutions along the x-z plane at $y = 0$ when $\lambda = \xi = 1$. The * indicates the location of the one-half monopole.

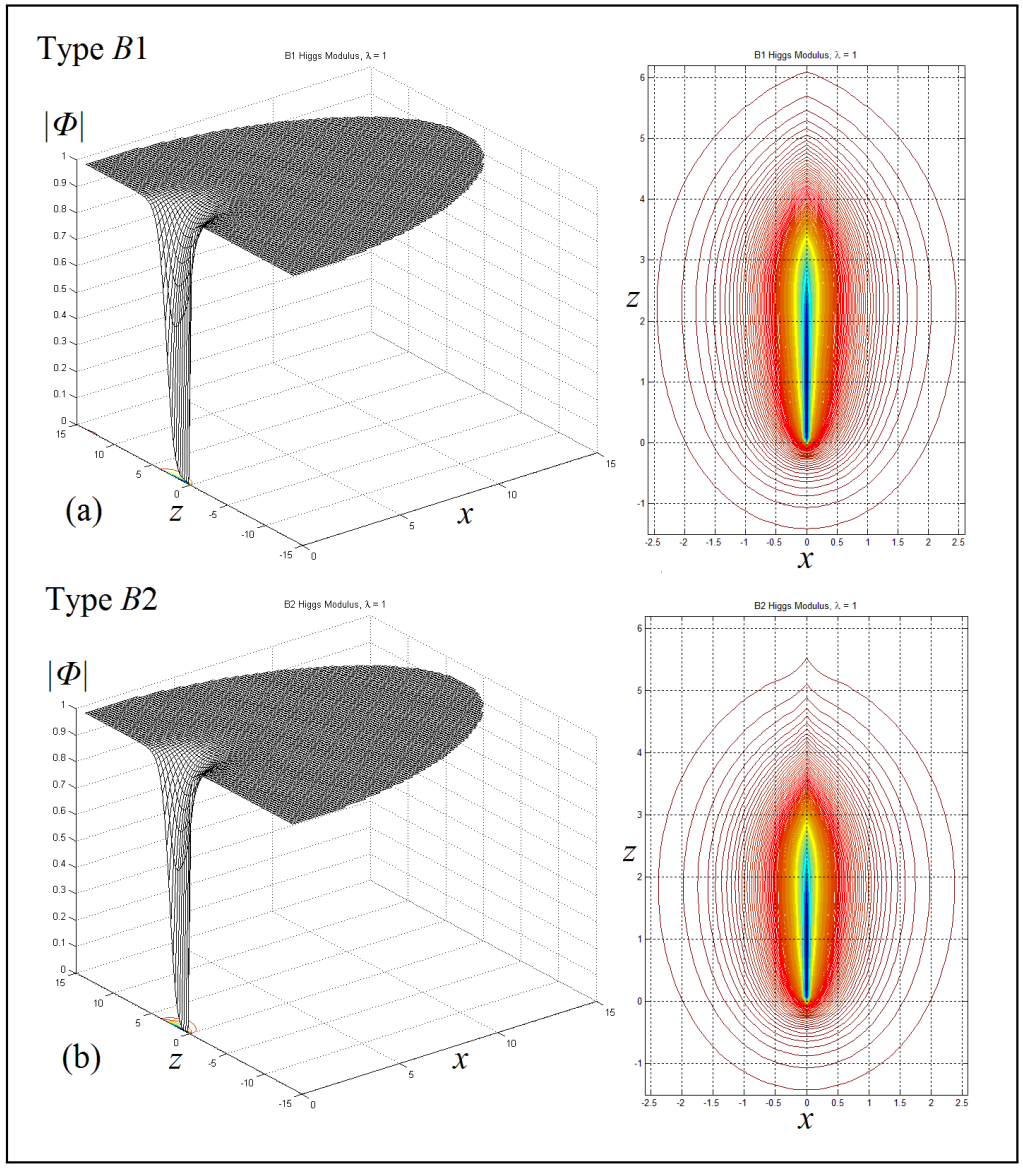

Figure 4: The 3D surface and contour plots of the Higgs field modulus $|\Phi|$ of the (a) Type $B1$ and (b) Type $B2$ one-half monopole solutions along the x-z plane at $y = 0$ when $\lambda = \xi = 1$.

The Energy Density and Total Energy

- The total dimensionless energy (12) of the Type 1 one-half monopole solutions is 0.509 and that of the Type 2 solutions is 0.525 when $\lambda = 0$. Their total energies are higher than the BPS total energy of a one-half monopole which is $\frac{1}{2}$.
- The total energies of the one-half monopole solutions are plotted versus $\lambda^{1/2}$ and $\ln(1+\lambda)$ for values $0 \geq \lambda \geq 12$. Figure 1 (c), (d). For a particular value of λ, the Type 2 solutions possess higher total energy compared to the Type 1 solutions.
- The total dimensionless energy (12) when ξ=g=1, can be written as

$$E = \int \mathcal{E} d\theta \; dr, \quad \mathcal{E} = \frac{1}{4} r^2 \sin\theta \{ B_i^a B_i^a + D_i \Phi^a D_i \Phi^a + \frac{\lambda}{2} (\Phi^a \Phi^a - \xi^2)^2 \}, \quad (50)$$

where $\mathcal{E}$ is the energy density. The 3D surface and contour line plots of $\mathcal{E}$ of the one-half monopole solutions along the x-z plane at $y = 0$ when $\lambda = 1$ are shown in Figure 5. The shape of the one-half monopole is that of a rugby ball.

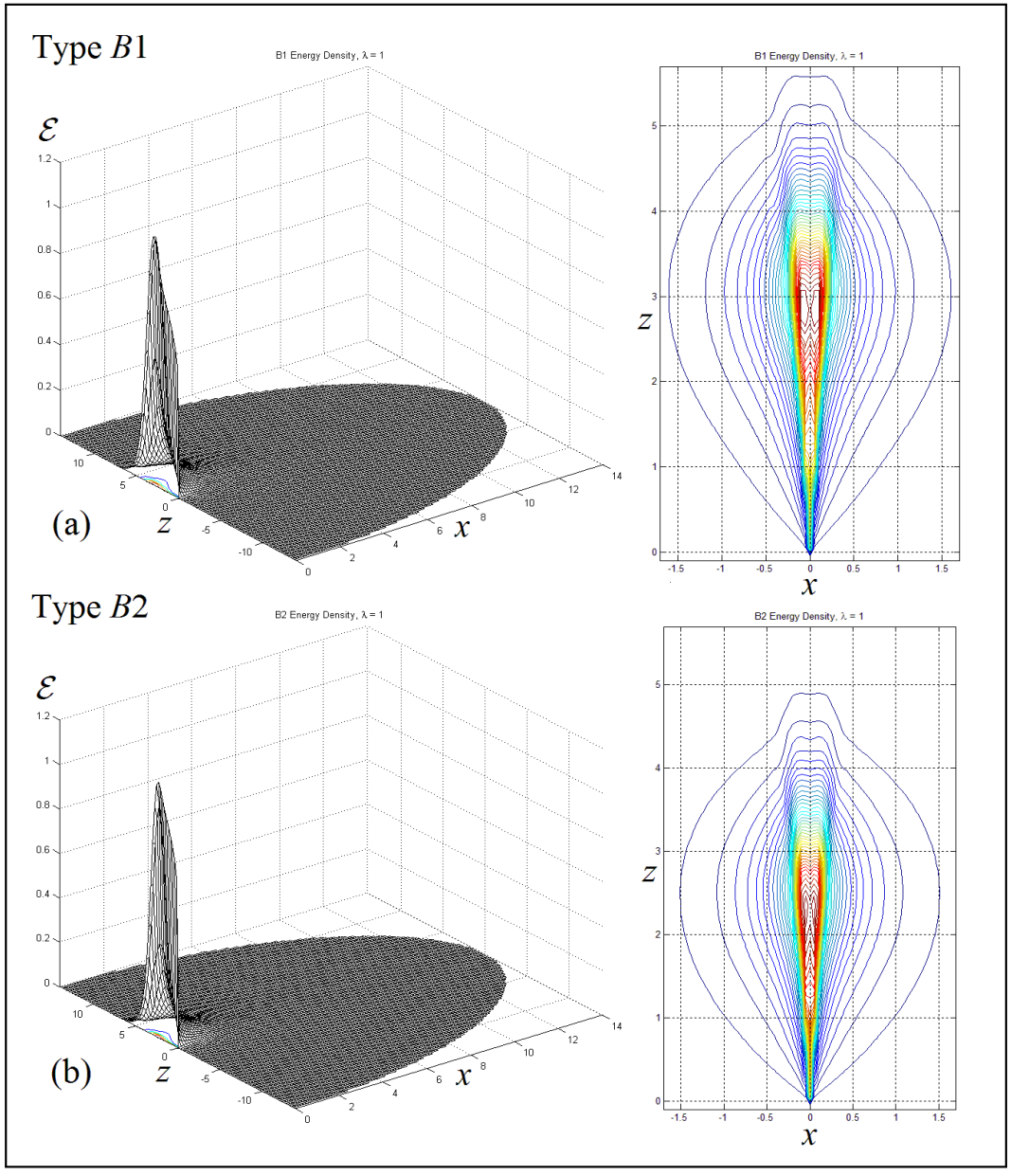

Figure 5: 3D surface and contour plots of the energy density $\mathcal{E}$ of the (a) Type $B1$ and (b) Type $B2$ one-half monopole solutions along the x-z plane at $y = 0$ when $\lambda = \xi = 1$.

Remarks

- From our analysis of the four one-half monopole solutions, we are able to conclude that the Type B solutions are exact 180^o rotation of the z-axis about $r = 0$ of the respective Type A solutions in 3D space. Hence they are gauge equivalent.
- We have found two different one-half monopole, the Type 1 and Type 2, as they are not gauge equivalent along the boundary at $\theta = \pi$ for the Type A solutions and along the boundary at $\theta = 0$ for the Type B solutions. These solutions are distinct in the region where the energy of the one-half monopole is concentrated.

Acknowledgments

Acknowledgments

The authors would like to thank the Universiti Sains Malaysia for the RU research grant (account Number: 1001/PFIZIK/811180) and the ICHEP 2012 conference organizer for the hospitality.

References

[1] G. 't Hooft, Nucl. Phy. **B79**, 276 (1974); A.M. Polyakov, Sov. Phys. - JETP **41**, 988 (1975); Phys. Lett. **B59**, 82 (1975); JETP Lett. **20**, 194 (1974).

[2] E.B. Bogomol'nyi and M.S. Marinov, Sov. J. Nucl. Phys. **23**, 357 (1976).

[3] M.K. Prasad and C.M. Sommerfield, Phys. Rev. Lett. **35**, 760 (1975); E.B. Bogomol'nyi, Sov. J. Nucl. Phys. **24**, 449 (1976).

[4] C. Rebbi and P. Rossi, Phys. Rev. **D22**, 2010 (1980); R.S. Ward, Commun. Math. Phys. **79**, 317 (1981); P. Forgacs, Z. Horvarth and L. Palla, Phys. Lett. **B99**, 232 (1981); Nucl. Phys. **B192**, 141 (1981); M.K. Prasad, Commun. Math. Phys. **80**, 137 (1981); M.K. Prasad and P. Rossi, Phys. Rev. **D24**, 2182 (1981).

[5] E.J. Weinberg and A.H. Guth, Phys. Rev. **D14**, 1660 (1976).

[6] Rosy Teh and K.M. Wong, J. Math. Phys. **46**, 082301 (2005); Int. J. Mod. Phys. **A20**, 4291 (2005).

References (cont.)

[7] P.M. Sutcliffe, Int. J. Mod. Phys. **A12**, 4663 (1997); C.J. Houghton, N.S. Manton and P.M. Sutcliffe, Nucl.Phys. **B510**, 507 (1998).

[8] B. Kleihaus and J. Kunz, Phys. Rev. **D61**, 025003 (2000); B. Kleihaus, J. Kunz, and Y. Shnir, Phys. Lett. **B570**, 237, (2003); B. Kleihaus, J. Kunz, and Y. Shnir, Phys. Rev. **D68**, 101701 (2003); Phys. Rev. **D70**, 065010 (2004).

[9] Rosy Teh, K.G. Lim and P.W. Koh, AIP Conference Proceedings Volume **1150**, 424 (2009).

[10] E. Harikumar, I. Mitra, and H.S. Sharatchandra, Phys. Lett. **B557**, 303 (2003).

[11] Rosy Teh and K.M. Wong, *Half-Monopole and Multimonopole*, Int. J. Mod. Phys. **A20**, 2195 (2005).

[12] N.S. Manton, Nucl. Phys. (N.Y.) **B126**, 525 (1977).

[13] J. Arafune, P.G.O. Freund, and C.J. Goebel, J. Math. Phys. **16**, 433 (1975).

References (cont.)

[14] A. Actor, Rev. Mod. Phys. **51**, 461 (1979).

[15] S. Coleman, *New Phenomena in Subnuclear Physics*, Proc. 1975 Int. School of Physics 'Ettore Majorana', ed A Zichichi, New York Plenum, 297 (1975).

[16] L.D. Faddeev, *Nonlocal, Nonlinear and Nonrenormalisable Field Theories*, Proc. Int. Symp., Alushta, Dubna: Joint Institute for Nuclear Research, 207 (1976); Lett. Math. Phys. **1**, 289 (1976).

[18] D.G. Boulware et al., Phys. Rev. **D14**, 2708 (1976).

[19] K.G. Lim, Rosy Teh and K.M. Wong, J. Phys. G: Nucl. Part. Phys. **39**, 025002 (2012).

[20] Rosy Teh, B.L. Ng, and K.M. Wong, *Particles of One-Half Topological Charge*, ArXiv: submit/0409918 [hep-th] 3 Feb 2012.